AD NUMBER

ADB817993

LIMITATION CHANGES

TO:

Approved for public release; distribution is unlimited. Document partially illegible.

FROM:

Distribution authorized to DoD only; Administrative/Operational Use; 29 AUG 1949. Other requests shall be referred to Air Materiel Command, Wright-Patterson AFB, OH 45433. Pre-dates formal DoD distribution statements. Treat as DoD only. Document partially illegible.

AUTHORITY

PB159576, publicly available per U.S. Government Research Reports v37 n7 dtd 5 Apr 1962

HqATSC Form No. 80-507 (20 Jan 45)
(Old AAFMC-266)

ATI No. 64810

Total Number of Pages - 48

ARMY AIR FORCES
~~MATERIEL~~
AIR ~~TECHNICAL SERVICE~~ COMMAND

ENGINEERING DIVISION
MEMORANDUM REPORT ON

MCREXE54/LVL/OEB/pm

Date 29 August 1949

SUBJECT: The Mechanism of Jet Disintegration

OFFICE Equipment Laboratory

Contract or Order No.

SERIAL No. MCREXE-664-531B
GS-USAF-Wright Patterson No. 179

Expenditure Order No. 664-764

A. PURPOSE:

1. To investigate the mechanism of jet disintegration in order to derive mathematical relations for computing droplet sizes produced by insecticide spray equipment.

B. FACTUAL DATA:

2. The results of an investigation regarding the effect of droplet size on the kill rate of the insects sprayed is contained in Memorandum Report No. MCREXE-664-531, GS-USAF-Wright Patterson No. 127, dated 31 May 1948, Subject: "Dissemination of Insecticides". From this investigation it appears possible to predict the most effective droplet size when certain information is available regarding: (1) the lethal amount of insecticide per insect; (2) the habits and physical characteristics of the insects; and (3) the effect of certain meteorological conditions. It was believed appropriate to supplement that information with data providing a basis for designing spray equipment capable of producing the most effective size of droplets for any given set of conditions enumerated above. Appendix "A" of this report contains the results of a study which was made to provide that data. Theoretical considerations regarding the phenomena whereby small droplets are produced by jet disintegration are reviewed in that appendix and test results examined. A theory about the mechanisms of jet disintegration is developed, and a procedure is shown for calculating the originating droplet sizes.

3. A liquid jet leaving a nozzle is unstable, since its surface can be reduced by disintegrating into small droplets. The disintegration is initiated by the formation of waves within the liquid column. The volume included between two nodal points represents the droplet size. This droplet

travels with a certain velocity. If the surface tension of this droplet is great enough to stand the ram pressure, this droplet will maintain its shape (if no evaporation is assumed) and the liquid jet will disintegrate into droplets of uniform size. If the surface tension of the droplet is so small that it cannot stand the ram pressure this droplet will continuously change its shape and by doing so disintegrate into smaller droplets of different sizes so that a droplet spectrum results. The maximum droplet size is the original droplet size. The minimum droplet size apparently approaches molecular dimensions. The form of the droplet spectrum depends on the ratio between original (maximum) droplet size and stable droplet size.

4. The calculation of the wave length can be carried through on a pure theoretical basis if the rotationally symmetric disturbances of the jet are the most influential as is the case for example for a liquid jet in still air, i.e., solid injection by a simple round nozzle. The wave lengths can be appropriately represented by a dimensionless characteristic value ζ_{opt}, representing the ratio between jet (nozzle) circumference and wave length. The ζ_{opt} value is nearly constant for cases where the viscosity forces of the liquid are the most effective forces, i.e., for comparatively small velocities of the jet. In these cases the droplet size is stable so that the liquid jet disintegrates into droplets of uniform size. The droplet diameter is approximately 2.4 times the jet diameter.

5. For higher jet velocities the resulting original droplet size in most cases will be unstable so that a droplet spectrum results. The maximum droplet of the spectrum is proportional to the jet diameter and inversely proportional to the cubic root of the characteristic value ζ_{opt}, the size of which depends on the liquid, the surrounding medium, the velocity, and the jet diameter. The volume of the maximum droplet is proportional to the capillary constant, proportional to the square of the jet diameter, inversely proportional to the density of the air and inversely proportional to the square of the jet velocity.

6. The characteristics of the spectrum can be computed by applying the laws of probability.

7. By comparing the calculated values with available test results, a good conformity has been found.

8. It is almost certain that the disintegration taking place in an ordinary carburator, i.e., liquid jet velocity very slow and high air velocity, can be calculated by the relations stated for solid injection,

since for the wave length only the difference between liquid velocity and the velocity of the surrounding medium is of importance. So by taking as velocity the difference between air velocity and liquid velocity, correct results should be obtained. Unfortunately, no proof can be given since in the available test results the nozzle diameter has not been stated.

9. All the above statements can be true only as long as rotationally symmetric disturbances of the liquid jet are of the most importance for the disintegration. With the kind of nozzle as used for spraying insecticides from an airplane (straight discharge type nozzle) the liquid jet is deflected about 90° directly after leaving the nozzle. This bending represents a strong singular disturbance of the jet so that the rotationally symmetric disturbances are of little influence for the disintegration. It is very unlikely that the wave length resulting from this singular disturbance can be calculated on a pure theoretical basis within a reasonable length of time. Test results show that the maximum droplet size resulting from the disintegration of a jet after leaving a nozzle under the above conditions is 4 to 8 times smaller than the maximum droplet size which would result from rotationally symmetric disturbances.

C. CONCLUSIONS:

10. It is very probable that by imprinting a definite wave length on the jet by outer forces, for example by mechanical vibration of the nozzle, the liquid will disintegrate into a certain droplet size if the outer forces are strong enough to overcome the other forces acting on the jet. So it may be possible to produce uniform droplet sizes where normally a droplet spectrum would result, provided that this droplet size is small enough to be stable.

11. The most important value for calculating the droplet sizes resulting from the disintegration of a liquid jet is the wave length originating in the liquid jet as a consequence of its instability.

12. In all cases where the rotationally symmetric disturbances are of minor influences, no exact relations could be stated as a consequence of the lack of detailed information and the lack of suitable test facilities. According to the available test results for cases where the liquid jet is deflected directly behind the nozzle, the singular disturbance caused by the bending is of major influence, resulting in smaller droplets than produced by rotationally symmetric disturbances.

Memorandum Report No. MCREXE-661-531B
GS-USAF-Wright Patterson No. 179
29 August 1949

D. RECOMMENDATIONS:

None - Data merely submitted.

O. E. Balje'
O. E. BALJE'

Prepared by L. V. LARSON
(Name)

Approved by E. M. HUNTINGTON, Lt. Col., USAF
Chief, Mechanical Branch

Approved by J. C. HARVELL, Colonel, USAF
for Chief, Equipment Laboratory
Engineering Division

Concurrence:

Distribution: (19)
Director of Intelligence,
Deputy Chief of Staff-Operations,
AFOIN
MCIAXF
MCID (2) "Release"
AFMEN3A, Mr. Muller
BAGR-CD (4)
AMC Engineering Field Officer, Bldg. "M",
Navy Department, Washington, D. C.
Naval Air Station, Jacksonville,
Florida, Attn: Lt. Comdr.
J. M. Hirst
Department of Agriculture, Bureau of
Entomology and Plant Quarantine,
Washington, D. C., Attn: Dr. Bishop
Dept. of Agriculture, Div. of Forest Insects
Investigations, Beltsville Lab., Beltsville, Md.
Deputy Chief of Staff-Surgeon General,
Preventive Medicine Branch, Attn: Maj. L. C. Kossuth
University of Florida, Gainesville, Fla.,
Attn: Mr. Charles R. Pearson
MCREXE5 (4)

APPENDIX A

Calculations About Droplet Sizes Produced by Simple Spray Nozzles

I. INTRODUCTION

1. It is a well known fact that any liquid stream disintegrates into droplets after leaving a nozzle or orifice. These droplets in some cases are of uniform size, in other cases of different sizes. The disintegration can be caused by many different influences, the details of which are very difficult to follow and are not yet completely clarified in current literature. Therefore, no relation for the produced droplet size could be found in the available literature except some approximation formulae which, however, unfortunately are either dimensionally incorrect or unsatisfactory in results (Ref. 1, 2, 3, 4). This seems to indicate that the most decisive influences governing the droplet sizes are not yet determined with sufficient accuracy even though innumerable tests and theoretical work has been devoted to the problem. In this report an attempt is made to develop a theory about the mechanism of jet disintegration, and to state a procedure for calculating the resulting droplet sizes.

II. THEORETICAL CONSIDERATIONS

1. A general relation for the droplet size may be derived according to Prandtl (Ref. 5) by considering the behavior of the free surfaces of liquids. The free surface of a liquid shows the tendency to reduce itself as much as possible. That tendency can be explained by assuming that each particle near to the surface is drawn to the interior of the liquid by the attractive forces of its neighbors. Therefore, only as many particles remain on the surface as are needed to inclose the fluid volume. As a consequence, certain tensions can be assumed to exist on the curved surface of a liquid, similar to the tensions in an uniformly stretched membrane. This tension is called surface tension or capillary tension. In plane surfaces these tensions do not exist and in this case the liquid is in equilibrium. However, for curved surfaces these tensions produce a pressure within the liquid which exceeds that of the surrounding atmosphere.

2. Considering a small rectangle on a curved surface with the sides ds_1 and ds_2, Figure 1, the pressure difference $p_1 - p_2$ on the area $ds_1 ds_2$ results in a force $(p_1 - p_2)ds_1 ds_2$. The surface tension causes two forces Cds_1 on the sides ds_1 and two forces Cds_2 on the sides ds_2 when C denotes the tension on the unit length (C = Capillary constant). These forces Cds_1 and Cds_2 have components normal to the surface $Cds_1 ds_2/R_2$ and $Cds_2 ds_1/R_1$ (being $d\alpha = ds_1/R_1$ and $d\beta = ds_2/R_2$, Figure 1) where R_1 and R_2 denote the radii. For the equilibrium it follows:

$$P_1 - P_2 = C\left(\frac{1}{R_1} + \frac{1}{R_2}\right) \quad (1)$$

For a sphere, $R_1 = R_2$ and therefore:

$$P_1 - P_2 = \frac{2C}{R} = \frac{4C}{d} \quad (2)$$

Equation 2 represents the relationship between droplet diameter, d, surface tension (or $p_1 - p_2$) and capillary constant, C.

3. When a liquid sphere moves through the atmosphere it is well known that the ram pressure, Δp, on the front of the sphere is proportional to the square of the flight speed, v, and directly proportional to the mass density of the air. That is:

$$\Delta p = \frac{v^2 \gamma_A}{2g} = \frac{1}{2}\rho_A v^2 \quad (3)$$

It is obvious that for the case where the ram pressure is higher than the surface tension, the flying droplet cannot withstand that pressure and will be deformed. Equilibrium will be established when:

$$\Delta p = p_1 - p_2 \quad (4)$$

Equation 4 can be regarded as a criterion which governs the maximum possible stable droplet size. Introducing equation 2 and 3 into Equation 4 results in:

$$d_{st} = \frac{8Cg}{\gamma_A v^2} = \frac{8C}{\rho_A v^2} \quad (5)$$

when, v, denotes the relative velocity between the droplet and the surrounding air. Table 1 shows the values of the capillary constant for several liquids against air of 295°K and 760 mm Hg (Ref. 6); and Figure 2 represents Equation 5 for T = 295°K, and an atmospheric pressure of 760 mm Hg. So Figure 2 shows the maximum possible droplet diameter which can exist for various velocities in air at 295°K and 760 mm Hg.

Liquid	C (kg/m)
Gasoline	$2.1\ 10^{-3}$
Water	$6.8\ 10^{-3}$
Ethyl alcohol	$2.4\ 10^{-3}$
Diesel fuel No. I	$2.7\ 10^{-3}$
Diesel fuel No. II	$2.8\ 10^{-3}$
Lubricating oil	$3.1\ 10^{-3}$

Table 1

4. Equation 5 shows that d_{st} depends mainly on the capillary constant and on the relative velocity, v. It can be assumed that, v, is either the velocity of the liquid jet and the surrounding air is at rest or that, v, is the velocity of the air and the liquid is at rest. A typical example of jet disintegration produced by liquid in motion and air at rest is the ordinary solid injection used in connection with Diesel engines. A typical example of jet disintegration produced by high velocity air in contact with a liquid at rest is the ordinary carburator used in connection with internal combustion engines. It may be mentioned that for solid injection, very high liquid pressures are required. The relation between liquid velocity and pressure is given by the relation:

$$v = \sqrt{\frac{2g\ \Delta p}{\gamma_L}} = \sqrt{\frac{2\ \Delta p}{\rho_L}} \qquad (6)$$

γ_L denoting the specific weight of the liquid. In Figure 2 the corresponding pressures, Δp, for different liquids, as given by Equation 6, are plotted on the velocity scale. Table 2 shows the values of the specific weight for several liquids (T = 295°K).

Liquid	γ_L [kg/m^3]
Gasoline	700
Water	1000
Ethyl alcohol	740
Diesel fuel	850
Lubricating oil	850

Table 2

5. By investigating the phenomena accompanying the disintegration by solid injection, it is possible to arrive at some clues about the influences governing the droplet sizes, besides the stability of the droplets. As shown by Lord Raleigh (Ref. 7), a cylindrical column of liquid is statically unstable as a consequence of the surface tension, since its surface can be reduced by disintegrating into droplets. The surface of a cylindrical jet is:

$$S_j = \pi\, dj \cdot L + \frac{\pi\, dj^2}{2} \tag{7}$$

when L denotes its length and dj the jet diameter. The volume is:

$$V_j = \frac{\pi\, dj^2\, L}{4} \tag{8}$$

If this volume disintegrates into droplets, the surface of the droplets becomes:

$$S_d = \frac{3\pi\, L\, d^2_j}{2 d_d} \tag{9}$$

and the ratio between the jet surface and the surface of the droplet is:

$$\frac{S_j}{S_d} = \frac{d_d}{1.5\, d_j} \left(1 + \frac{d_j}{2L} \right) \tag{10}$$

i.e., for a jet of infinite length ($L = \infty$) the surface of the jet is greater than the surface of the droplets, if the droplet diameter is greater than $1.5\, d_j$, for $d_j = L$ the surface of the jet is greater than the surface of the droplets if the droplet diameter is greater than the jet diameter and for $d_j > L$ the surface of the jet is greater, even if the droplet diameter is smaller than the jet diameter. The transition to the disintegration is induced by the fact that irregularities of the column occur, produced by the nozzle itself or outer forces. The surface tension causes the pressure inside the thinner region to become higher than inside the wider region (compare Equation 1) so that the liquid content is forced into the thicker spaces of the column. So the thinner region becomes thinner and thinner, and finally the column disintegrates into droplets. It suggests itself

that the droplet diameter can be calculated if the volume enclosed between two thinner regions (nodal points) is known, i.e., if the wave length within the liquid column is known. A theoretical investigation for the wave length is made by C. Weber (Ref. 5), and is reviewed in the following paragraph.

6. Investigated is a cylindrical liquid column of infinite length without considering the attractive force of the earth. If the surface of such a column shows a slight deviation, δ, from its originally cylindrical shape, Figure 3, the whole column will be disturbed by wavelike motions which cause the liquid column to disintegrate. Establishing the equation for the equilibrium of the column for the above conditions by applying the Navier-Stokes equations yields a differential equation which can be solved by assuming a certain function for the deviation as:

$$\delta = \delta_0 e^{\mu t} \cos \xi \frac{x}{a} \tag{11}$$

when ξ denotes the ratio between jet circumference and wave length,

$$\xi = \frac{2\pi a}{\lambda} = \frac{d_N \pi}{\lambda} \tag{12}$$

a, denotes the radius of the jet which can be assumed proportional to the nozzle radius, $\frac{d_N}{2}$. The value, x, in Equation 11 denotes the coordinate in the direction of the jet axis and δ a function of r, which must be equal to $\bar{\delta}$, for r = a, if $\bar{\delta}$ represents a characteristic value for the average deviation, Figure 3. It has been shown that only the rotationally symmetric disturbances are decisive for the disintegration, i.e., δ is independent of φ (see Fig. 3), if no strong unsymmetrical outer forces are acting on the jet, i.e., for a liquid column in still air. An approximate solution of the above differential equation is:

$$\mu^2 = \frac{c_R}{2 \gamma_L a^3} (1 - \xi^2) \xi^2 \tag{13}$$

whereby μ represents a characteristic value for the disintegration time

$$t = \frac{\ln a/\bar{\delta}}{\mu} \tag{14}$$

Equation 13 shows that there is a definite relation between the characteristic value, ξ, representing the wave length, and the μ value, representing the disintegration time, Figure 4. It is pointed out by C. Weber that only those wave lengths the μ value of which is the maximum are decisive for the disintegration. These values may be denoted with the subscript "opt". So it finally results that ξ_{opt} represents a relation for the wave length determining the droplet size. This value can be calculated from Equation 13 by applying well known mathematical transformations.

Equation 13 can be true only if the surface tension is the most influential factor governing the wave length. For viscous liquids the viscosity must also be taken into account. For this case equation 13 can be written in the form:

$$\mu = -\frac{3\eta g}{2\gamma_L a^2}\zeta^2 \pm \sqrt{\frac{\eta g}{2\gamma_L a^3}(1-\zeta^2)\zeta^2 + \left(\frac{3\eta g}{2\gamma_L a^2}\zeta^2\right)^2} \qquad (15)$$

which results in:

$$\mu_{opt} = \left(\sqrt{\frac{8\gamma_L}{Cg}}\, a^{1.5} + \frac{6\eta}{C}\, a\right)^{-1} \qquad (16)$$

and:

$$\zeta_{opt} = \left[2\left(1+\sqrt{\frac{9\eta^2 g}{2C\gamma_L a}}\right)\right]^{-0.5} \qquad (17)$$

For the case where aerodynamic forces have to be considered (higher jet velocities) the relation between, μ, and, ζ, takes the form:

$$\mu^2 + \mu\frac{3\eta g}{\gamma_L a^2}\zeta^2 = \frac{Cg}{2\gamma_L a^3}(1-\zeta^2)\zeta^2 + \frac{\gamma_A v^2}{2\gamma_L a^2}\zeta^3 f_0(\zeta) \qquad (18)$$

In Equation 18, $f_0(\zeta)$ denotes a Bessel-function as represented in Figure 5. C. Weber points out that above certain velocities a wave formation as shown in Figure 6 can exist for which the relation reads:

$$\mu^2 + \mu\frac{\eta\zeta^2 g}{1.2\gamma_L a^2}\left[\frac{3\frac{\eta\zeta^2 g}{\gamma_L a^2} + \mu}{\frac{10}{3}\frac{\eta g}{\gamma_L a^2} + 3\frac{\eta\zeta^2 g}{\gamma_L a^2} + \mu}\right] = \frac{\gamma_A v^2}{\gamma_L a^2}\zeta f_1(\zeta) - \frac{2Cg}{a^3\gamma_L}\zeta^2 \qquad (19)$$

In Equation 19, $f_1(\zeta)$ denotes another Bessel-function also as represented in Figure 5. It must be mentioned that Equations 18 and 19 can be true only as long as the air can be regarded as incompressible, i.e., as long as, v, is considerably smaller than the velocity of sound. The velocity above

which the wave formation as shown in Figure 6 can exist is given by:

$$V_{min} = \sqrt{\frac{2C_g}{a^2 \gamma_A} \frac{\xi}{f_1(\xi)}} \tag{20}$$

since the right part of Equation 19 must be at least zero.
From the above relations the disintegration length can be calculated since:

$$l = vt \tag{21}$$

7. It has been shown by A. Haenlein (Ref. 9) that the relationships as stated by C. Weber give an approximately true picture of the main influences governing the disintegration of a liquid jet. A. Haenlein was mostly concerned with the disintegration time and the disintegration length of a liquid jet at relatively small velocities and states that in many cases the values as calculated by C. Weber agree with the values as found by tests, and that in some other cases, however, no agreement could be found.

8. With the considerations as represented in paragraph 6, the volume of a droplet becomes:

$$V = \frac{d_d^3 \lambda}{4} \tag{22}$$

By using Equation 12, the relation for the droplet diameter becomes:

$$d_d = \frac{d_j \sqrt{\frac{3\pi}{2}}}{\sqrt[3]{\xi_{opt}}} \tag{23}$$

9. For calculating the droplet sizes the values ξ_{opt} must be derived from Equation 18. ξ_{opt} is the ξ value for which the maximum μ value results. Equation 18 can be written in the form:

$$\mu^2 - \mu \frac{3\eta g}{\gamma_L a^2} \xi^2 - \frac{C_g}{2\gamma_L a^3} (1-\xi^2) \xi^2 - \frac{\gamma_A v^2}{2\gamma_L a^2} \xi^3 f_0(\xi) = 0 \tag{24}$$

and solved for, μ, resulting in:

$$\mu = -\frac{3\eta g}{2\gamma_L a^2}\zeta^2 \pm \frac{1}{2}\sqrt{\left(\frac{3\eta g}{2\gamma_L a^2}\zeta^2\right)^2 + 4\left[\frac{Cg}{2\gamma_L a^3}(1-\zeta^2)\zeta^2 + \frac{\gamma_A V^2}{2\gamma_L a^2}\zeta^3 f_0(\zeta)\right]} \quad (25)$$

From Equation 25 the maximum of, μ, can be found by differentiating. This yields the equation for the value, ζ_{opt}, which reads:

$$\pm \zeta^6 A \pm \zeta^5 B - \zeta^4 C - \zeta^3 D - \zeta^2 E = 0 \quad (26)$$

with:

$$A = \frac{27\eta^4 g^2}{16\gamma_L^2 a^4} - \frac{2Cg}{\gamma_L a^3}$$

$$B = \left(\frac{27\eta^4 g^2}{8\gamma_L^2 a^4} - \frac{4Cg}{\gamma_L a^3}\right)\frac{\gamma_A V^2}{\gamma_L a^2}\frac{f_0(\zeta)}{\delta\zeta}$$

$$C = \frac{9\eta^2 g^3 C}{2\gamma_L^3 a^7} \pm \frac{\gamma_A^4 V^4}{\gamma_L^4 a^4}\left(\frac{f_0(\zeta)}{\delta\zeta}\right)^2 \pm \frac{27\eta^2 Cg^3}{8a^5\gamma_L^3} - \frac{4C^2 g^2}{\gamma_L^2 a^6} + \frac{81\eta^4 g^4}{16\gamma_L^4 a^8}$$

$$D = \frac{9\gamma_A V^2 \eta^2 g^2}{\gamma_L^3 a^6} f_0(\zeta) \pm \frac{2Cg^3\eta^2}{\gamma_L^3 a^6}\frac{f_0(\zeta)}{\delta\zeta}$$

$$E = \frac{9\eta^4 g^3 C}{2\gamma_L^3 a^7} \pm \frac{\gamma_A^2 V^4}{\gamma_L^2 a^4 4}$$

The exact solution of this equation is not possible in an explicit form. However, the calculations show that in many cases the influence of the viscosity is very small, especially at higher velocities, so that the second term on the left side in Equation 18 can be omitted. Then the differentiated Equation 18 reads:

$$\frac{\delta\mu}{\delta\zeta} = \pm \frac{\frac{Cg}{2\gamma_L a^3}\zeta - \frac{Cg}{\gamma_L a^3}\zeta^3 + \frac{3\gamma_A V^2 z_0 \zeta^2}{4\gamma_L a}}{\sqrt{\frac{Cg}{2\gamma_L a^3}(1-\zeta^2)\zeta^2 + \frac{\gamma_A V^2}{2\gamma_L a^2}\zeta^3 z_0}} \quad (27)$$

In Equation 27 the value, s_0, represents $f_0(\xi)$, and can be considered constant and equal to one at higher jet velocities (see Fig. 5). From Equation 27 it follows for ξ_{opt}:

$$\pm\left[\xi^3 - \xi^2 \frac{3\gamma_A v^2 a z_0}{4Cg} - \frac{\xi}{2}\right] = 0 \tag{28}$$

Equation 28 is an irreducible case, and cannot be solved by Cardan's formula, but must be solved with trigonometric functions. This gives:

$$y_1 = 2\sqrt{\left(\frac{3\gamma_A v^2 a z_0}{4Cg}\right)^2 \frac{1}{9} + \frac{1}{6}} \cos\frac{\varphi}{3} \tag{29}$$

$$y_2 = 2\sqrt{\left(\frac{3\gamma_A v^2 a z_0}{4Cg}\right)^2 \frac{1}{9} + \frac{1}{6}} \cos\frac{\varphi + 2\pi}{3} \tag{30}$$

$$y_3 = 2\sqrt{\left(\frac{3\gamma_A v^2 a z_0}{4Cg}\right)^2 \frac{1}{9} + \frac{1}{6}} \cos\frac{\varphi + 4\pi}{3} \tag{31}$$

$$\cos\varphi = \frac{\frac{2}{27}\left(\frac{3\gamma_A v^2 a z_0}{4Cg}\right)^2 + \frac{1}{6}\left(\frac{3\gamma_A v^2 a z_0}{4Cg}\right)}{2\sqrt{\frac{\left(\frac{3\gamma_A v^2 a z_0}{4Cg}\right)^6}{730} + \frac{\left(\frac{3\gamma_A v^2 a z_0}{4Cg}\right)^4}{162} + \frac{\left(\frac{3\gamma_A v^2 a z_0}{4Cg}\right)^2}{108} + \frac{1}{216}}} \tag{32}$$

So it results that Equation 28 cannot be solved in an explicit form. Only for the case $\xi_{opt} \gg 1$, an explicite approximate solution results since then Equation 18 can be written in the form:

$$\mu = \pm\sqrt{\xi^3 f_0(\xi)\frac{\gamma_A v^2}{2\gamma_L a^2} - \xi^4 \frac{Cg}{2\gamma_L a^3}} \tag{33}$$

Appendix A

Differentiating Equation 33, [redacted] gives:

$$\frac{\delta\mu}{\delta\xi} = \pm \frac{\frac{3\gamma_A v^2 z_o}{4\gamma_L a^2}\xi^2 - \frac{c_g \xi^3}{\gamma_L a^3}}{\sqrt{\xi^3 z_o \frac{\gamma_A v^2}{2\gamma_L a^2} - \xi^4 \frac{c_g}{2\gamma_L a^3}}} \tag{34}$$

and for ξ_{opt}:

$$\xi^3 - \frac{3\gamma_A v^2 a z_o}{4c_g}\xi^2 = 0 \tag{35}$$

Reducing Equation 35 by Cardan's substituion:

$$\xi = \gamma + \frac{\gamma_A v^2 a z_o}{4c_g} \tag{36}$$

$$\gamma = \frac{2\gamma_A v^2 a z_o}{4c_g} \tag{37}$$

$$\xi_{opt} = \frac{3\gamma_A v^2 a z_o}{4c_g} = \frac{3}{4} z_o Z \tag{38}$$

In Equation 38 the term

$$Z = \frac{\gamma_A v^2 a}{c_g} \tag{39}$$

represents a dimensionless characteristic value for the disintegration of a liquid jet at high velocities.

10. For calculating the wave length in the case of wave formation according to Figure 6, Equation 19 must be developed for ξ_{opt}. For an exact solution, Equation 19 must be written in the form of an equation of the third degree resulting in:

$$\mu^3 + \mu^2 A + \mu B + C = 0 \tag{40}$$

with:

$$A = \frac{\eta g}{\gamma_L a^2}\left(\frac{\xi^2}{1.2} + 3\xi^2 + \frac{10}{3}\right)$$

$$B = \frac{\eta^2 g^2 \xi^4 3}{1.2\,\gamma_L^2 a^4} - \frac{\xi}{a^2 \gamma_L}\left(\gamma_A v^2 f_1(\xi) - \frac{2 c_g \xi}{a}\right)$$

$$C = -\frac{\eta g}{\gamma_L a^2}\left(3\xi^2 + \frac{10}{3}\right)$$

By reducing Equation 40 by applying Cardom's substitution, an equation of the 12 degree would have to be solved for obtaining the value, μ, in an explicit form as needed for the determination of the desired value, ξ_{opt}. However, by considering Equation 19, it appears justified for greater values of, μ, to omit the part in parenthesis, so that Equation 19 is reduced to a quadratic equation. Solving this equation for, μ, results in:

$$\mu = \pm\frac{1}{2}\sqrt{\xi^4 \frac{\eta^2 g^2}{\gamma_L^2 1.2^2 a^4} + \xi^2 \frac{8 c_g}{\gamma_L a^3} - \frac{4\gamma_A v^2}{\gamma_L a^2}\xi f_1(\xi) - \xi^2 \frac{\eta g}{\gamma_L 1.2\, a^2}} \qquad (41)$$

Differentiating Equation 41, it results for ξ_{opt}:

$$-\xi^6 \frac{3\eta^4 g^4}{1.2^4 \gamma_L^4 a^8} - \xi^4 \frac{24\eta^2 c_g^3}{1.2^2 \gamma_L^3 a^7} + \xi^3 \frac{14\eta^2 g^2 \gamma_A z_1 v^2}{1.2^2 \gamma_L^3 a^6}$$
$$+\xi^2 \frac{16 c_g^2 g^2}{\gamma_L^2 a^6} - \xi \frac{8 c_g \gamma_A z_1 v^2}{\gamma_L^2 a^5} + \frac{\gamma_A^2 z_1^2 v^4}{\gamma_L^2 a^4} = 0 \qquad (42)$$

In Equation 42, s_1 denotes $f_1(\xi)$ which value can be considered constant and equal to one at high velocities (see Fig. 5). Equation 42 is an equation of the 6 degree and cannot be solved in an exact manner in an explicit form of ξ. Only for the case that the viscosity is neglected completely as may be justified for higher velocities, an explicit solution for ξ results. In this case, Equation 19 can be written in the form:

$$\mu = \pm\sqrt{\frac{\gamma_A v^2}{\gamma_L a^2}\xi f_1(\xi) - \frac{2 c_g}{a^3 \gamma_L}\xi^2} \qquad (43)$$

Appendix A

Differentiating Equation 43 gives, ζ_{opt}

$$\zeta_{opt} = \frac{\gamma_A v^2 a z_1}{4 c_g} = \frac{Z z_1}{4} \tag{44}$$

11. It must be mentioned that by wave formation according to Figure 6, no definite statement about the droplet size can be made since it is not possible to predict in which places the liquid column will break off. This most probably will happen at points with a distance of $\lambda/2$, for which case the droplet diameter will become:

$$d_d = \frac{d_j \sqrt{\frac{3\pi}{2}}}{\sqrt[4]{2 \zeta_{opt}}} \tag{45}$$

but might as well happen at other points as influenced by outer forces on the liquid column.

12. From the considerations as represented in paragraphs 9 and 11, a definite statement about the droplet size can be made only up to a certain limit as determined by Equation 20, i.e., as long as the velocity does not exceed a certain value. Below this limit, Equation 38 in connection with Equation 23 can be used for determining the droplet size resulting from the disintegration of a jet at medium velocities and Equation 17 in connection with Equation 23 for small velocities. For intermediate velocities, Equation 38 does not give exact values as a consequence of the simplification involved in the derivation of the equation. In those cases, the original Equation 18 (or the slightly simplified Equation 28) should be used. Figure 7 shows the difference of the values obtained with the above equations, indicating that the exact Equation 18 has to be applied only within a relatively small range. So for higher jet velocities a direct relation for the droplet size can be stated by introducing Equation 38 into Equation 23, which gives:

$$d_d = 3.02 \sqrt[3]{\frac{c_g d_j^2}{\gamma_A v^2}} = \frac{2.4\, d_j}{\sqrt[3]{Z}} \tag{46}$$

For small velocities, Equation 17 can be simplified, since the term under the root in that equation is of little influence to the result, so that for this case the relation for the droplet diameter reads:

$$d_d = 2.44\, d_j \tag{47}$$

Figure 8 shows a graphical representation of Equations 46 and 47, from which the droplet diameter can be found as a function of the jet diameter, d_j, (in the most cases equal to the nozzle diameter, d_N) and the velocity, v, for Diesel Oil No. 1 in air of 295°K and 760 mm Hg. Similar diagrams can be plotted for any other conditions by applying the above relations.

13. Equation 5 represents the relation for the maximum possible stable droplet size. Obviously for the case that the droplet diameter becomes greater (according to Fig. 8) than indicated by Equation 5, the originating droplet cannot be stable and will be deformed. This deformation occurs in a form as indicated in Figure 9. The droplet will be dented and lingaments will be formed which travel along, continuously changing its shape. As outer forces are acting on these lingaments, they will disintegrate into smaller parts so that finally a variety of droplet sizes, a droplet spectrum, will result. However, some lingaments will travel along undisturbed being protected from the aerodynamic forces by other lingaments so that some droplets will have the original size. It can be predicted that in cases where the velocity is greater than given by Equation 5, a droplet spectrum will result, the maximum droplet diameter of which can be calculated according to Equation 46 and represented in Figure 8. The theoretical limit for stability is indicated by a thin solid line denoted by the number one. $(V_{max}/V_{stable} = 1)$

14. Calculations about the droplet spectrum can be performed by applying the laws of probability. The rate of probability, P, is the ratio of the favorable cases, f, to possible cases, p.

$$P = \frac{f}{p} \qquad (48)$$

The number of faverable cases and possible cases can be calculated by considering the possible combinations. This may be demonstrated by an example. The maximum droplet may have the volume, V_{max}. In many cases, as described in the foregoing paragraph, this droplet diameter is unstable since the surface tension cannot withstand the ram pressure. So the droplet will disintegrate. It may be assumed that the stable droplet diameter for the prevailing conditions has a volume of $V_{max}/4$. So the maximum number into which the droplet probably will disintegrate is four and the original droplet diameter with the volume, V_{max}, may be thought of as consisting of four units, each having the size, $V_{max}/4$. Now it may be considered how many combinations can be formed by a droplet of the size V_{max} having a tendency to disintegrate into four equal parts. By calculating the possible

combinations it has to be kept in mind that there is no inevitable necessity to disintegrate always just into four droplets, since the original droplet may be protected in some cases by other droplets in such a manner that it disintegrates into three or two droplets or does not disintegrate at all. If the droplet disintegrates into two droplets the combinations as listed in Table 3 are possible. If the droplet disintegrates into three droplets the combinations as listed in Table 4 are possible.

First Droplet	Second Droplet
1 unit	3 units
2 units	2 units
3 units	1 unit

Table 3

First Droplet	Second Droplet	Third Droplet
1 unit	1 unit	2 units
1 unit	2 units	1 unit
2 units	1 unit	1 unit

Table 4

If the droplet disintegrates into four droplets, four droplets result each having the size of one unit and for the case that the droplet does not disintegrate, one droplet of the size of four units results. By summarizing all these combinations it results that there is only one favorable case that one droplet results the size of which then is four units, i.e., the original size. Two favorable cases for droplets of the size three units, five favorable cases for droplets of two units and twelve favorable cases for droplets consisting of one unit can be found. Summarizing all the favorable cases one obtains the number of possible cases, i.e., $1 + 2 + 5 + 12 = 20$. So, according to Equation 48, the rate of probability that droplets of the size one unit will be formed is $12/20 = .60$, i.e., 60% of the dispersed amount is converted into droplets of the size one unit. The rate of probability that droplets of the size two or less units will be formed is $\frac{12 + 5}{20} = .85$, i.e., 85% of the total dispersed volume is

converted into droplets of the size two or less units and $\frac{12 + 5 + 2}{20}$ = .95, i.e., 95% into droplets of the size three or less units and $\frac{12 + 5 + 2 + 1}{20}$ = 100% into droplets of the size four or less units. Instead of terms of unit volume, the above figures can be written in terms of droplet diameter, since $d = 2\sqrt{\frac{V}{\text{const.}}}$ and one unit = $V_{max}/4$ = .63 d_{max}, 2 units = $2V_{max}/4$ = .795 d_{max}, three units = $3V_{max}/4$ = .91 d_{max} and four units = V_{max} = d_{max}. So, the droplet spectrum can be represented by a diagram showing droplet size in terms of maximum droplet diameter as a function of the quantity converted into droplets having the indicated or a smaller diameter, Figure 10.

15. It must be mentioned that the stable droplet diameter is not the smallest possible droplet diameter as would follow from the considerations presented in paragraph 14. In paragraph 6 it has been shown that a variety of wave lengths can exist, of which the wave length as represented by ζ_{opt} is of the strongest influence determining the maximum droplet size. However, that does not mean that the smaller wave lengths disappear completely, only their influence is of smaller degree. Especially on the outer surface of the liquid column these smaller wave lengths can produce some droplets the size of which is even smaller than the stable droplet size. Furthermore, vibrations not produced by the instability of the liquid column itself but from outer forces and disturbances in the nozzle itself may produce very small droplets the smallest of which may even approach molecular dimensions. It will be assumed that the percentage of volume converted into these small droplets (smaller than stable size) decreases with decreasing droplet diameters and that the function between volume converted and droplet size for droplets below stable size probably will show a tendency reciprocal to the tendency derived for droplet sizes above stable size (see paragraph 14) as indicated by a dotted line in Figure 10. In some cases the droplet spectrum is represented by a diagram showing the number of droplets, Z , as a function of the droplet diameter. This kind of spectrum can be calculated from Figure 10 by converting the ordinate of Figure 10 into number of droplets by using:

$$Z = \frac{\% \text{ Volume}}{d^3} \cdot \text{const.} \qquad (49)$$

With this relation it will be found that the maximum number of droplets of one size results for droplet sizes below stable size. A further investigation of the value, Z_{max}, may be omitted since this value probably is of little significance for the consideration of spray equipment since very small droplets have little chance to settle on the ground because of the vertical convection in the air.

16. The considerations as presented in paragraph 14 can be applied for any value of the ratio, V_{max}/V_{stable}. The calculations show that the number of cases are represented by a sequence:

1 2 5 12 28 64 144 320 697 1518

so that, for example, for the case that the original droplet disintegrates into eight pieces the values are as represented in Table 5. It follows that different droplet spectra result, depending on the ratio, V_{max}/V_{stable} or $(d_{max}/d_{stable})^3$. This ratio also can be represented approximately by:

$$\frac{V_{max}}{V_{stable}} = \left(\frac{d_{max}}{d_{stable}}\right)^3 = 0.216\ z^2 \qquad (50)$$

according to Equation 46 and 5 (see Fig. 8). It must be mentioned that the different droplet spectra probably are not directly proportional to the characteristic value, d_{max}/d_{stable}, and this value will have to be multiplied by a factor which is smaller than one and decreases with increasing velocities, since in determining the stable droplet size the velocity prevailing at the originating points of the stable droplets has to be considered, i.e., a velocity at a location behind the disintegration of the jet. This velocity is smaller than the initial velocity of the jet and is not known exactly.

Size of Unit	Number of Cases	Volume Percentages	d/d_{max}
1/8	320	$\frac{320}{576} = .555$	.5
2/8	144	$\frac{320+144}{576} = .805$	.64
3/8	64	$\frac{320+144+64}{576} = .916$	.722
4/8	28	.965	.795
5/8	12	.985	.855
6/8	5	.994	.91
7/8	2	.999	.96
8/8	1	1.0	1.0
	576		

Table 5

17. It must be mentioned that the velocity, v, in all the above equations denotes the actual jet velocity (or relative velocity) at the originating points of the droplets. This velocity in some cases might be very close to the exit velocity, c, from the nozzle; in many other cases might differ considerably from the exit velocity as a consequence of the losses. For calculating these losses, it might be assumed that the relations valid for the resistance of globules can be applied, since the jet starts its wave formation directly behind the nozzle, so that the shape of the jet is more similar to a sequence of globules than to a cylinder. The air resistance of a globule is:

$$R = \frac{D\,A\,\gamma_A\,v^2}{2g} \tag{51}$$

When D denotes a drag coefficient dependent on the Reynolds Number and A the projected area of the globule, The deceleration of the droplet is:

$$b = \frac{R}{m} \tag{52}$$

when, m, denotes the mass of the globule. Introducing Equation 51 into Equation 52, it follows for the deceleration.

$$b = \frac{0.75\,D\,v^2\,\gamma_A}{L\,d_d} \tag{53}$$

The actual velocity of the globule is:

$$v^2 = c^2 - 2bL \tag{54}$$

When, L, denotes the distance from the nozzle which in the following can be substituted by the disintegration length, l . Introducing Equation 53 into Equation 54, it results for the correction factor:

$$\xi = \frac{c}{v} = \sqrt{1 + \frac{1.5\,D\,\gamma_A\,l}{\gamma_L\,d_d}} \tag{55}$$

For the disintegration length, l , and droplet diameter, d_d, in case of small jet velocities, Equations 21, 14, 16 and 51 can be introduced into Equation 55, resulting in:

$$\xi = \sqrt{1 + \frac{\ln a/\delta\,\bar{v}\,D\,\gamma_A\,0.615\left(\sqrt{\frac{d_j\,\gamma_L}{cg}} + \frac{3\eta}{c}\right)}{\gamma_L}} \tag{56}$$

Appendix A

For high jet velocities it results by introducing Equations 21, 14, 33, 38 and 46 into Equation 55.

$$\xi = \sqrt{1 + \frac{\ln a/\delta^* D \sqrt{\gamma_A}\ 1.34}{Z^{1.166}\sqrt{\gamma_L}}} \qquad (57)$$

In equations 56 and 57, $\ln a/\delta^*$, is a factor the tendency of which is not well known. However, some clues about its probable value can be obtained by applying Equation 10, since this equation gives a definite relation for the maximum possible disintegration length. Equation 10 can be written in the form:

$$L = \frac{d_j}{\frac{3X d_j}{d_d} - 2} = 1 \qquad (58)$$

when X denotes the ratio of jet surface to droplets surface. According to the considerstion represented in paragraph 5, the factor X must be greater than 1 or at least be 1 . Introducing Equations 47, 21, 14 and 16 into Equation 58, it follows:

$$\ln a/\delta^* = \frac{1}{(1.23x - 2)\sqrt{\left(\sqrt{\frac{d_j \gamma_L}{c_g}} + \frac{3\eta}{c}\right)}} \qquad (59)$$

Equation 59 is valid for a jet with low velocities. For a jet with high velocities it results by introducing Equation 46, 21, 14, 33 and 38.

$$\ln a/\delta^* = \frac{0.465\, Z^{1.5}\sqrt{\gamma_A}}{(1.23x\sqrt[3]{Z} - 2)\sqrt{\gamma_L}} \qquad (60)$$

Equation 59 indicates that X has to be greater than 1.62 in order to give positive values of $\ln a/\delta^*$ and that then $\ln a/\delta^*$ is inversely proportional to the jet velocity. From Equation 60 no definite statement about the size of the factor X can be made since in the most cases where Equation 60 is applicable the value $\sqrt[3]{Z}$ is greater than 1.6. Introducing Equations 59 and 60 respectively into Equations 56 and 57 respectively, it results for the correction factor:

$$\xi = \sqrt{1 + \frac{D \gamma_A\ 0.615}{\gamma_L (1.23x - 2)}} \qquad (61)$$

valid for small jet velocities, and

$$\xi = \sqrt{1 + \frac{D\gamma_A \, 0.625 \, \sqrt[3]{Z}}{\gamma_L \, (1.25 \times \sqrt[3]{Z} - 2)}} \qquad (62)$$

valid for high jet velocitiss. So it results that the correction factor is proportional to the density of the air and inversely proportional to the density of the liquid. That means that the difference between the velocity in the nozzle and the velocity at the originating points of the droplets increases with increasing air densities and decreasing liquid densities. As a consequence of the losses, furthermore, the limit between disintegration into uniform droplet sizes and disintegrations into a variety of droplets is at higher velocities as indicated in Figure 8, if for the velocity the exit velocity from the nozzle is taken. In addition, the characteristic value, V_{max}/V_{stable} is affected by the losses if the velocity is referred to the exit velocity, i.e., the values, V_{max}/V_{stable} will be lower than indicated in Figure 8.

III. TEST RESULTS

1. Some test results about droplet sizes and droplet spectrum originating by disintegrating liquid jets (solid injection) are published by D. W. Lee and R. C. Spencer (Ref. 6). Table 6 represents the obtained maximum droplet sizes and Figure 11 some of the droplet spectra. The nozzles were simple round orifices.

2. For solid injection some photographic studies were performed on a liquid jet discharged through a simple round orifice with different velocities, Figure 12. These pictures show that at low velocities ($\Delta p < 30$ psi) uniform droplets originate, the diameter of which is about 2-1/2 times the jet diameter and that at higher velocities ($\Delta p > 30$ psi) a variety of droplet sizes originate.

3. F. N. Scheubel (Ref. 3) published test results concerning droplet sizes and droplet spectrum originating by the disintegration of a liquid jet discharged with very low velocity, into an airstream of very high velocity, Figure 13. Unfortunately, the nozzle diameter has not been stated.

Appendix A

No.	(m/s) V	(m) d_N	(kg/m) C	(kg/m3) γ_L	(kg sec/m²) η	($\frac{kg}{m^3}$) γ_A	(μ) d_{max}
1	119	2×10^{-4}	2.7×10^{-3}	850	2.20×10^{-4}	1.15	124
2	107	"	"	"	"	"	124
3	89	"	"	"	"	"	178
4	76	"	"	"	"	"	178
5	53	"	"	"	"	"	230
6	236	"	"	"	"	13.6	76
7	240	5.1×10^{-4}	"	"	"	15	86
8	101	"	"	"	"	13.6	146
9	240	"	2.6×10^{-3}	"	10.20×10^{-4}	15	102
10	89	2×10^{-4}	2.4×10^{-3}	740	11.5×10^{-4}	1.15	127
11	94	"	2.1×10^{-3}	700	42×10^{-6}	"	127
12	78	"	6.6×10^{-3}	1000	103×10^{-6}	"	276

Table 6

4. The nozzle type used for dispersing insecticide from airplanes is shown in Figure 14 (straight discharge nozzle). In this nozzle the liquid is discharged perpendicular to an high velocity airstream. The airstream deflects the liquid therein for about 90°. Test results with this nozzle type are represented in Table 7 and Figure 15.

No.	(m/sec) v	(m) d_M	(kg/m) C	(kg/m^3) γ_L	$(kg\ sec/m^2)$ η	(kg/m^3) γ_A	Appendix A (μ) d_{max}
1	90	6.36×10^{-3}	2.8×10^{-3}	850	1020×10^{-6}	1.15	325
2	90	2.54×10^{-2}	"	"	"		460
3	90	5.08×10^{-2}	"	"	"		810

Table 7

5. The droplet sizes in all the above test results were determined by allowing the droplets to settle on glass slides covered with magnesium oxyde. The droplets evaporate on these slides and leave marks. By measuring these marks under a microscope the droplet size can be found. The edges of these marks are not in all cases very distinguished, so that the obtained values are more or less arbitrary. This is shown by the fact that different institutions evaluating test slides sprayed in the same test report maximum droplet sizes which differ up to 100 %, (Ref. 10).

IV. COMPARISON BETWEEN TEST RESULTS AND CALCULATED VALUES

1. Figure 16 shows the comparison between the test values from Table 6 and the values calculated according to Equation 46, if for the velocity, v, the exit velocity, o, is taken. This figure shows that in all but four cases the test results are greater than the calculated values as it was to be expected according to the considerations represented in paragraph 16. This difference gives the chance to compute the size of the drag-coefficient, D. From Equation 46 it follows:

$$\left(\frac{d_{measured}}{d_{calculated}} \right)^3 = \frac{o^2}{v^2} \tag{63}$$

and, therefore, by introducing Equations 55 and 62:

$$D = \frac{\left[\left(\frac{d_{measured}}{d_{calculated}} \right)^3 - 1 \right] \left(1.25 \times \sqrt[3]{Z} - 2 \right) \gamma_L}{0.625 \sqrt[3]{Z}\ \gamma_A} \tag{64}$$

results.

Appendix A

Introducing the values from Figure 16 into Equation 60 for the drag coefficient values between 54 and 408 result (average value D = 192) for $\varkappa = 1$. The Reynolds numbers in the above cases are between 700 and 9000. According to the aerodynamic theory for the above Reynolds numbers, values between 0.4 and 0.5 were to be expected. For this difference several factors are responsible. From Equation 60 for $\ln \eta \delta^*$ under the prevailing conditions, values very close to zero result, indicating that the average deviation δ^* of the jet from its cylindrical shape is about equal to the jet radius, a. In addition, the value ξ_{opt} for the prevailing conditions is considerably greater than 1 (between 10 and 3000, see Equations 38 and 39), indicating that the wave length λ is much smaller than the jet diameter (3 to 1000 times, see Equation 12). Therefore, the outer shape of the liquid column is sharply deviated. It is not unlikely that the drag coefficient of such a sharply dented column is bigger than the drag coefficient of a globule. Furthermore, for the velocity, c, its theoretical value c_0 according to Equation 6 has been taken, since for the cited tests only the pressure difference was known. The coefficient of discharge representing the difference between the actual exit velocity and the theoretical value depends mainly on the kind of orifice and types of stem used for the test, which values, unfortunately, were not presented in the reports cited. They vary between $\frac{c}{c_0} = 0.94$ to 0.5 (Ref. 11). Finally, it must not be overlooked that the procedure of measuring droplet sizes is not very exact as mentioned in paragraph III.5.

2. Comparing some measured (solid lines in Fig. 17) droplet spectra, Figure 17, with the calculated spectra (dotted lines in Fig. 17), it results that the tendencies of the calculated and measured spectra are in fair agreement. However, the characteristic values V_{max}/V_{stable} of the measured spectra are much lower than those resulting from Figure 8. This again is a consequence of the losses since the jet velocity decreases considerably with increasing distances (see also Ref. 12). Therefore, the stable droplet size and the value V_{stable} increase and the value V_{max}/V_{stable} becomes lower than indicated in Figure 8. In Reference 6 it is shown that in distances of 7.5 inches from the nozzles still ligaments can be found. From Reference 12 it results that in air of atmospheric density the jet velocity in a distance of 7.5 inches from the nozzle is about 0.59 c_0. So the stable droplet size is about 2.9 times greater (see Equation 51) than suggested in Figure 8, and the value V_{max}/V_{stable} about 25 times smaller than suggested in Figure 8. With this correction measured and calculated spectrums are about identical.

3. The pictures represented in Figure 12 show that up to pressures of Δ_p = 20 psi (1.4 at), i.e., velocities of C = 19 m/s uniform droplet sizes result and at pressures above Δ_p = 30 psi (2.25 at), i.e., velocities above C = 24.5 m/s, a droplet spectrum results. According to Equations 39 and 50, the velocity which indicates the limit between disintegration into uniform droplets and droplet spectrums ($V_{max} = V_{stable}$) is given by:

$$V_K = 1.465 \sqrt{\frac{c\,q}{r_A\,a}} \qquad (65)$$

resulting in V_k = 10.4 m/s for the above case. This indicates that the velocity at the point where the original (maximum) droplet disintegrates further is between $\frac{10.4}{19}$ and $\frac{10.4}{24.5}$, i.e., between 55% and 43% of the exit velocity from the nozzle. That means according to Equations 50 and 39 that the actual value of $\frac{V_{max}}{V_{stable}}$ is between 0.55^2 and 0.43^2, i.e., between 30% and 18% of the theoretical value of $\frac{V_{max}}{V_{stable}}$. This has to be taken into account when using the exit velocity, c, by applying Figure 8 instead of using the actual velocity V, which in most cases will not be known.

4. For the conditions prevailing during the tests with the straight discharge nozzle as represented in Table 7, the calculated maximum droplet sizes are 1490μ, 3740μ and 5930μ for test No. 1, 2 and 3, by applying Equation 46, i.e., the calculated values are 4.6, 8.1 and 7.3 times greater than the measured values. It could not be expected that for this nozzle type even approximately correct values can be obtained by applying Equation 46 since for this nozzle type the disintegration probably is not caused by rotationally symmetric disturbances, but rather by the singular disturbance effected by the deflection of the jet. In order to calculate the wave length, i.e., the droplet size, for these conditions, more information about the size and the location of the irregular disturbances should be available.

APPENDIX B

Symbols

a	(m)	Radius of the jet
C	(kg/m)	Capillary constant
d_d	(m)	Droplet diameter
d_{max}	(m)	Maximum droplet diameter
d_j	(m)	Jet diameter
d_{st}	(m)	Stable droplet diameter
g	(m/sec^2)	Gravity constant
p	(kg/cm^2)	Pressure
T	(^0K)	Temperature
t	(sec)	Time
v	(m/sec)	Velocity
z		Dimensionless characteristic value
γ_A	(kg/m^3)	Specific weight of the air
γ_L	(kg/m^3)	Specific weight of the liquid
η	($kg\ sec/m^2$)	Dynamic viscosity
λ	(m)	Wave length
ξ		Characteristic value for the wave length
μ	(sec^{-1})	Characteristic value for the disintegration time

APPENDIX C

References

1. Nukiyama, S and Tanasawa, Y. Trans. Soc. Mech. Engrs. (Japan) 4, No. 14, 86 (1938); 4, No. 15 138 (1938); 5, No. 18, 63 (1939) 5, No. 18, 68 (1939); 6, No. 22, IL-7 (1940); 6, No. 23, IL-18 (1940)

2. Triebnigg, H. Der Einblase - und Einspritzvorgang bei Dieselmaschinen Springer (Vienna) 1925 (Solid injection for Diesel engines)

3. Scheubel, F. W. On atomization in carburators T. M. No. 644, NACA 1931.

4. Lewis, H. C. and Edwards, D. G. A study of the atomization of liquids, OSRD No. 6345 October 1945.

5. Prandtl, L. Ein Fuehrer durch die Stroemungslehre ZWB 1944 (Hydro and aerodynamics).

6. Lee, D. W. and Spencer, R. C. Photomicrographic studies of fuel sprays, Report No. 454 NACA 1933.

7. Lord Rayleigh, Proc. Lond. Math. Soc. 10 (1879) Page 4.

8. Weber, C. Zum Zerfall eines Fluessigkeitsstrahles. Z.f. angew. Math. u. Mech. Vol. 11, No. 2,1931 (On the disintegration of a liquid jet).

9. Haenlein, A. Disintegration of a liquid jet. Technical Memorandums No. 659 NACA 1932.

10. Naval Air Station, Patuxent River, Maryland. Development and test of airplane dispersal of DDT. Aerosol, Project No. TED No. PTR 32175, 29 January 1945.

11. Gelalles, A. G. Effect of orifice length-diameter ratio on spray characteristics. T.N. No. 352 NACA 1930.

12. Schweitzer, P. H. Penetration of Oil Sprays. Bulletin No. 46 of the Pennsylvania State College Engineering Experiment Station.

Appendix D

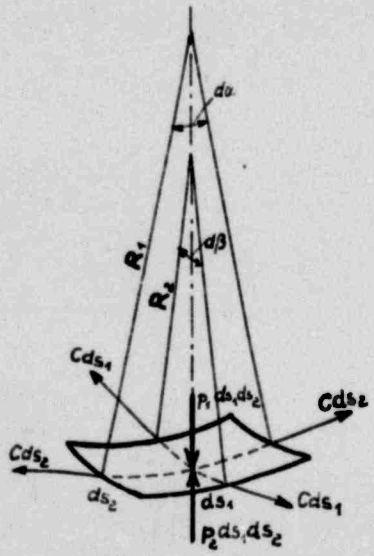

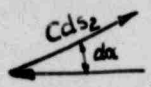

Fig. 1 Tensions on a curved surface

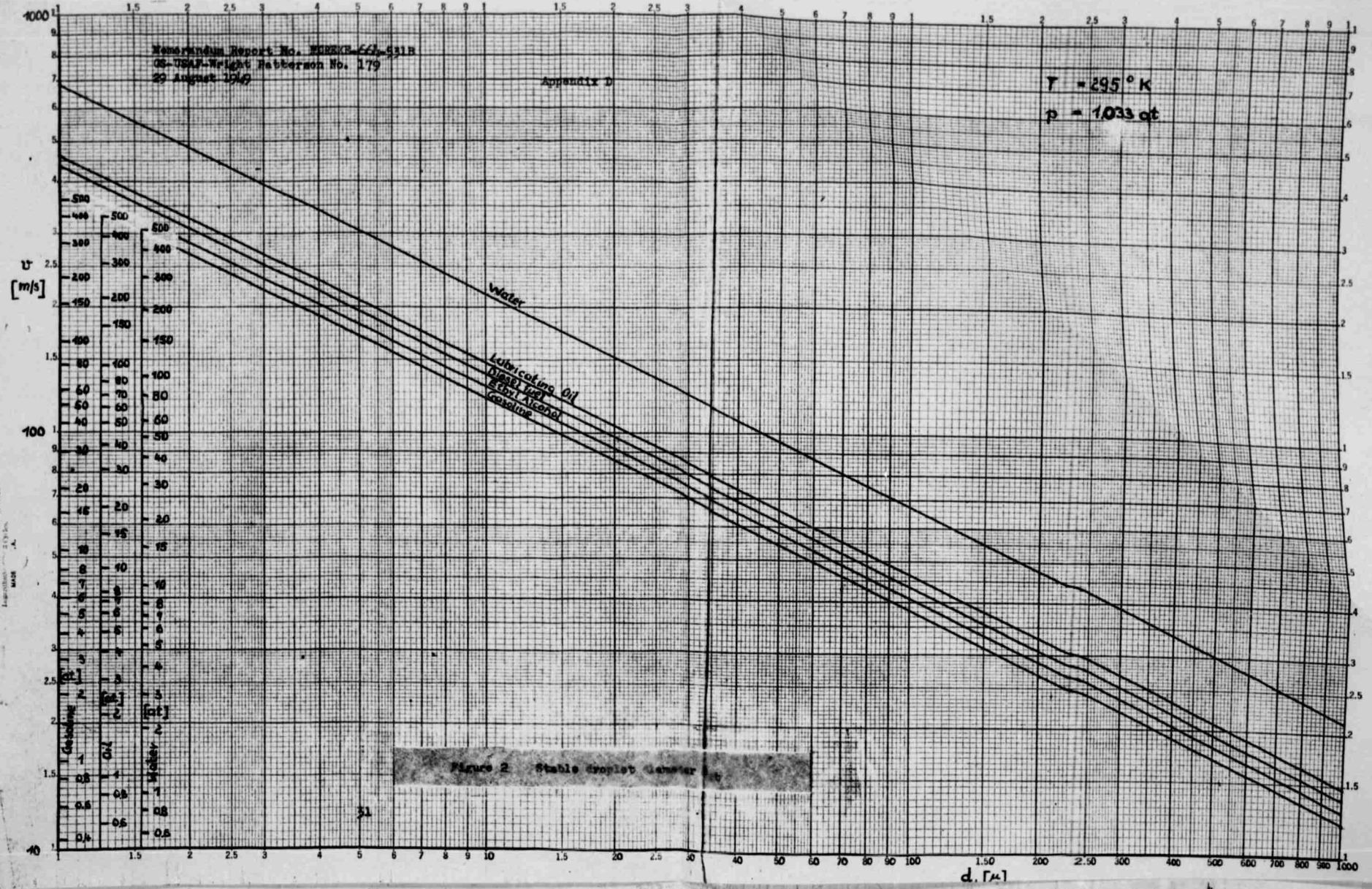

Figure 2 Stable droplet diameter [illegible]

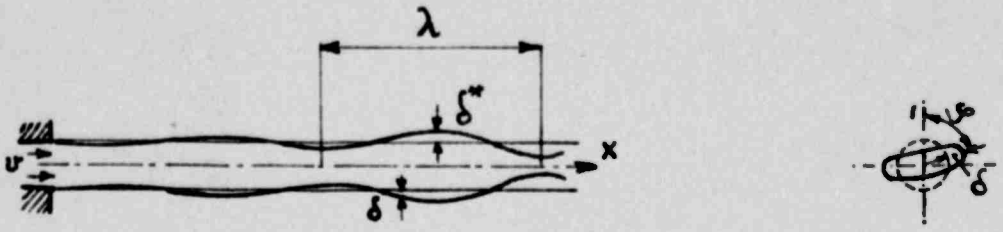

Fig. 3 Disintegration of a liquid jet.

Appendix D

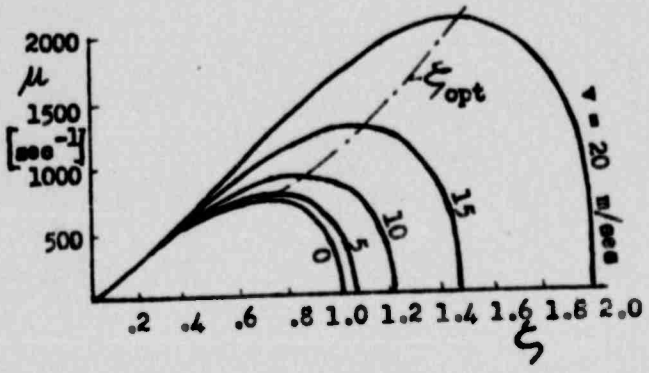

Fig. 4 Relation between μ and ξ for water (a = .00025 m)
(according to C.Weber [8])

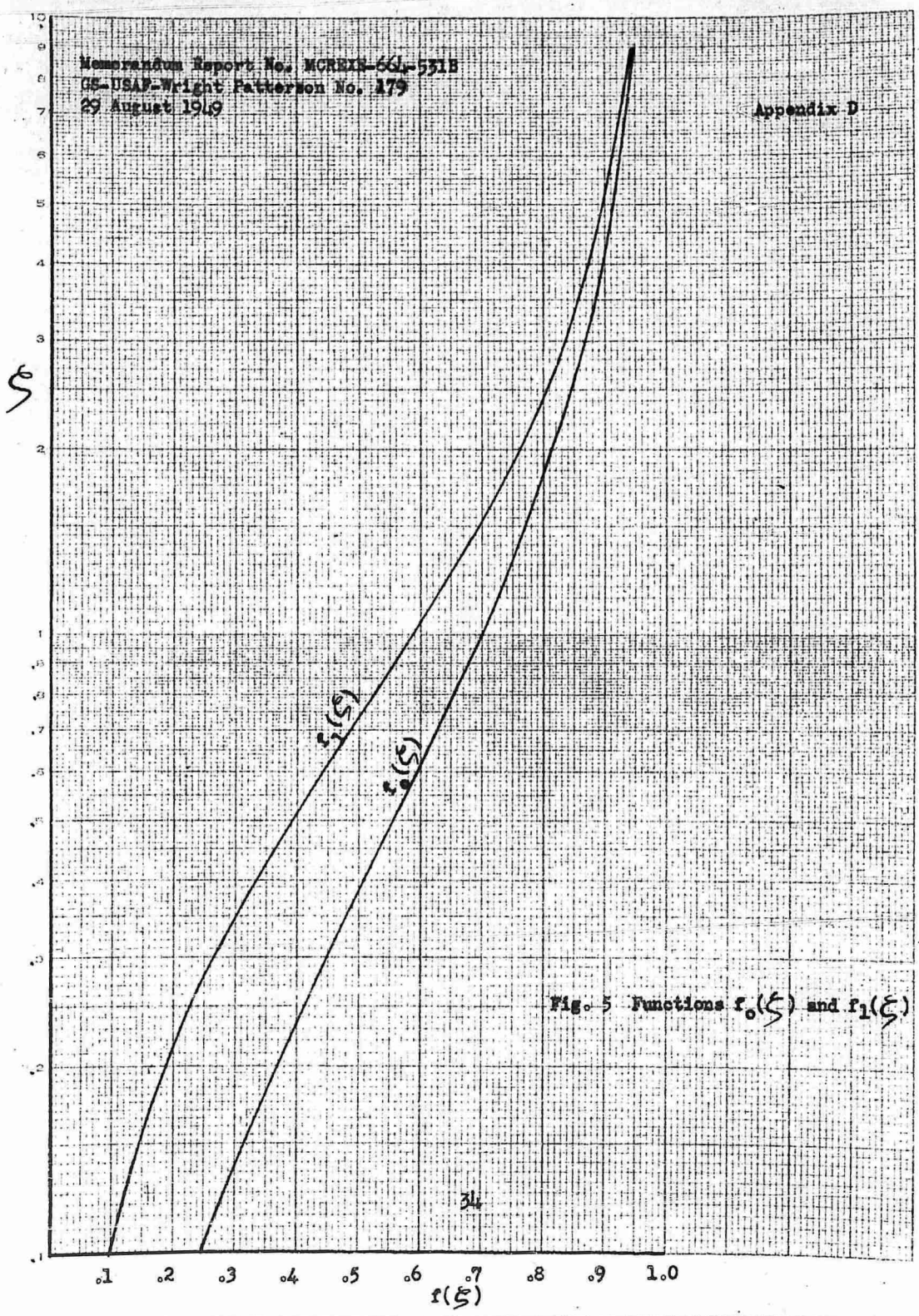

Fig. 5 Functions $f_0(\xi)$ and $f_1(\xi)$

Fig. 6 Wave formation

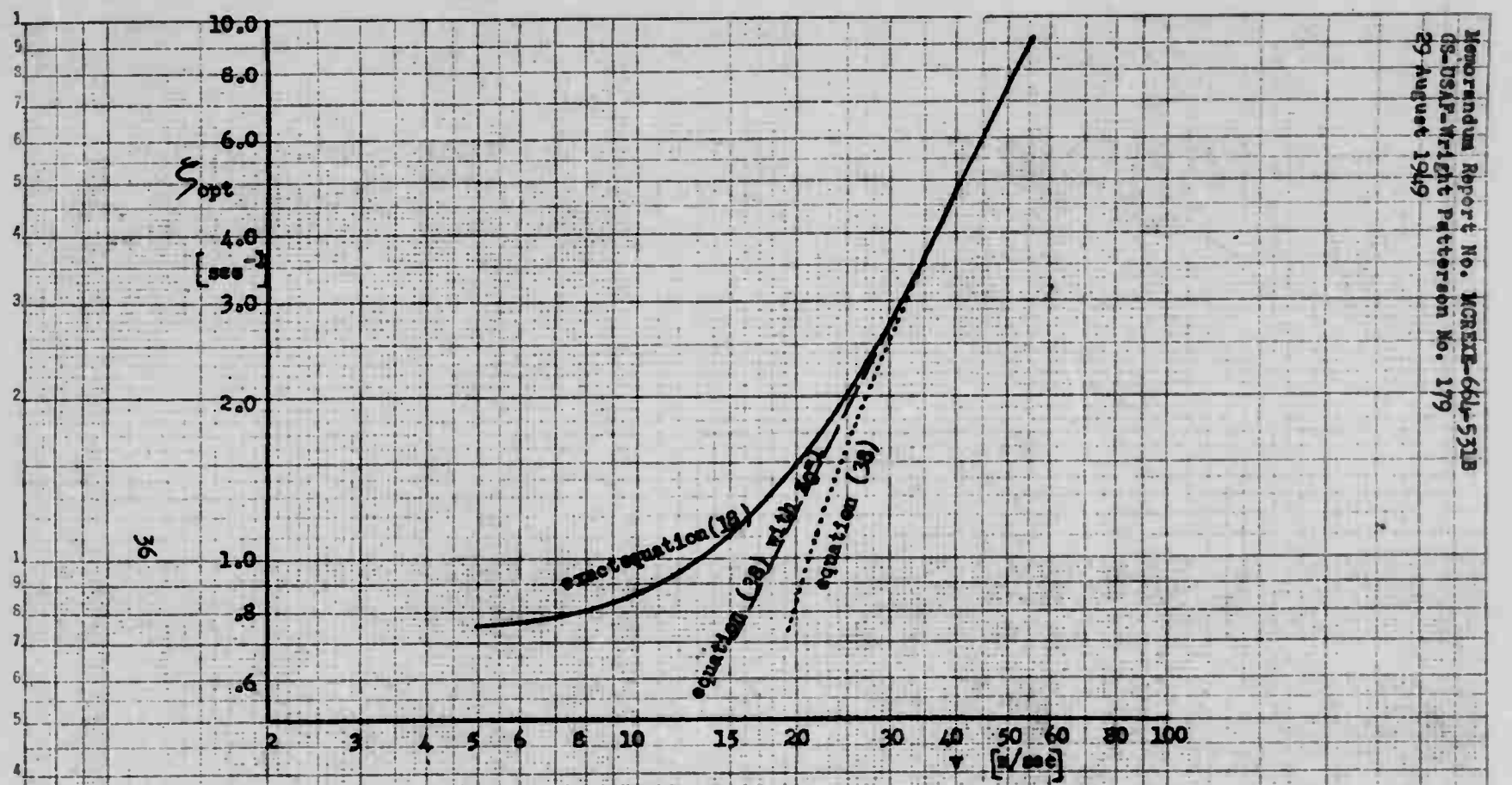

Fig. 7 Values obtained by Equations (18), (38) and equation (38) with z_0=1

Memorandum Report No. MCREXE-664-531B
GE-USAF-Wright Patterson No. 179
29 August 1949

Appendix D

Fig. 8 Relation between droplet diameter, Nozzle diameter and velocity.

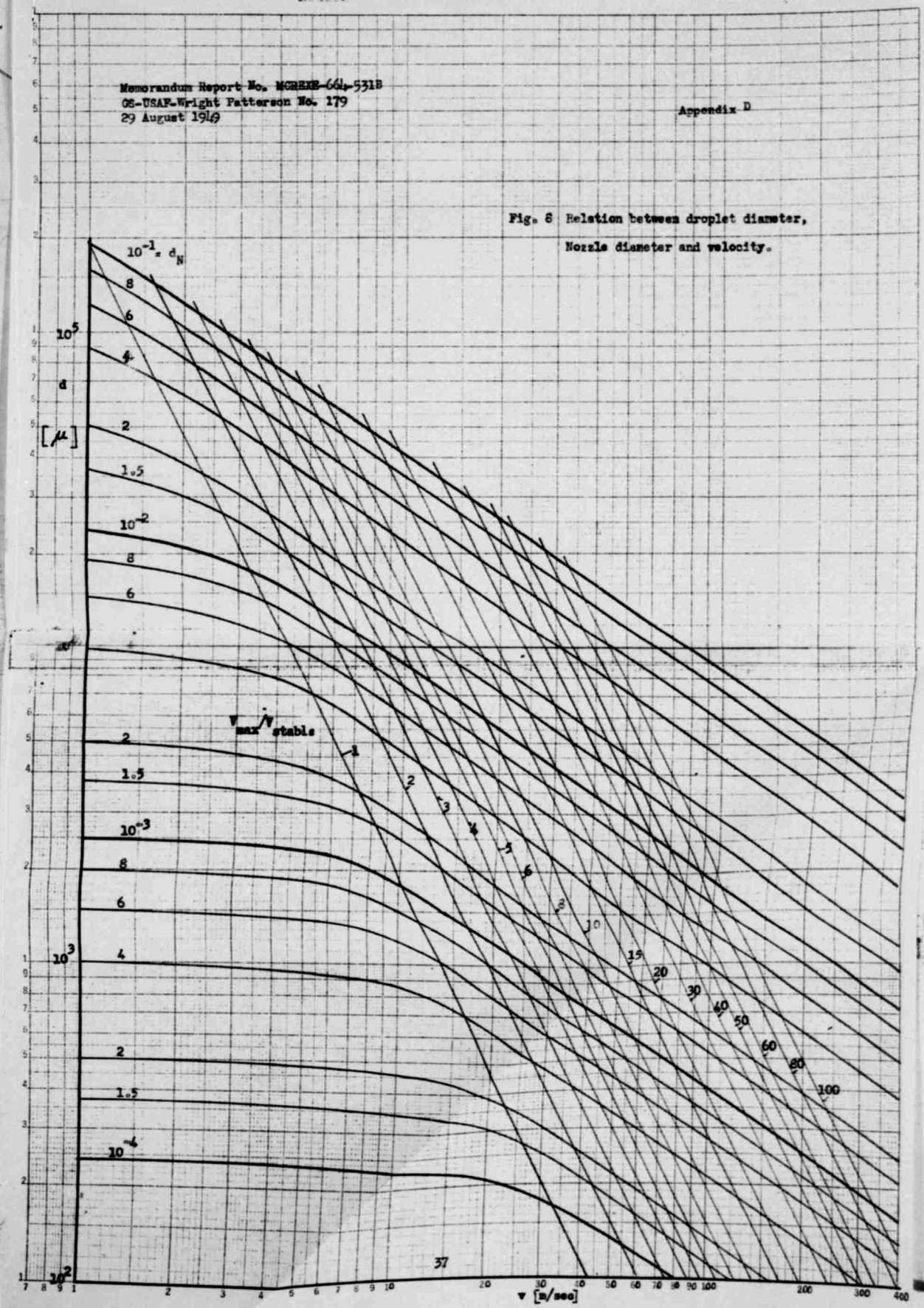

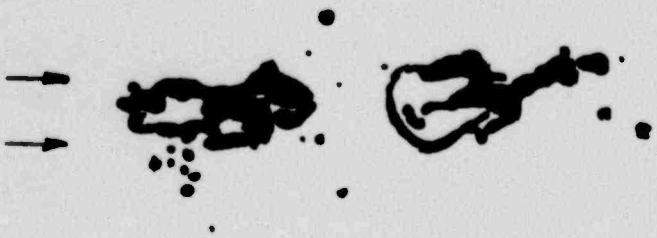

Fig. 9 Disintegrating droplet (according to pictures as published by D.W.Lee and R.C.Spencer [6])

Appendix D

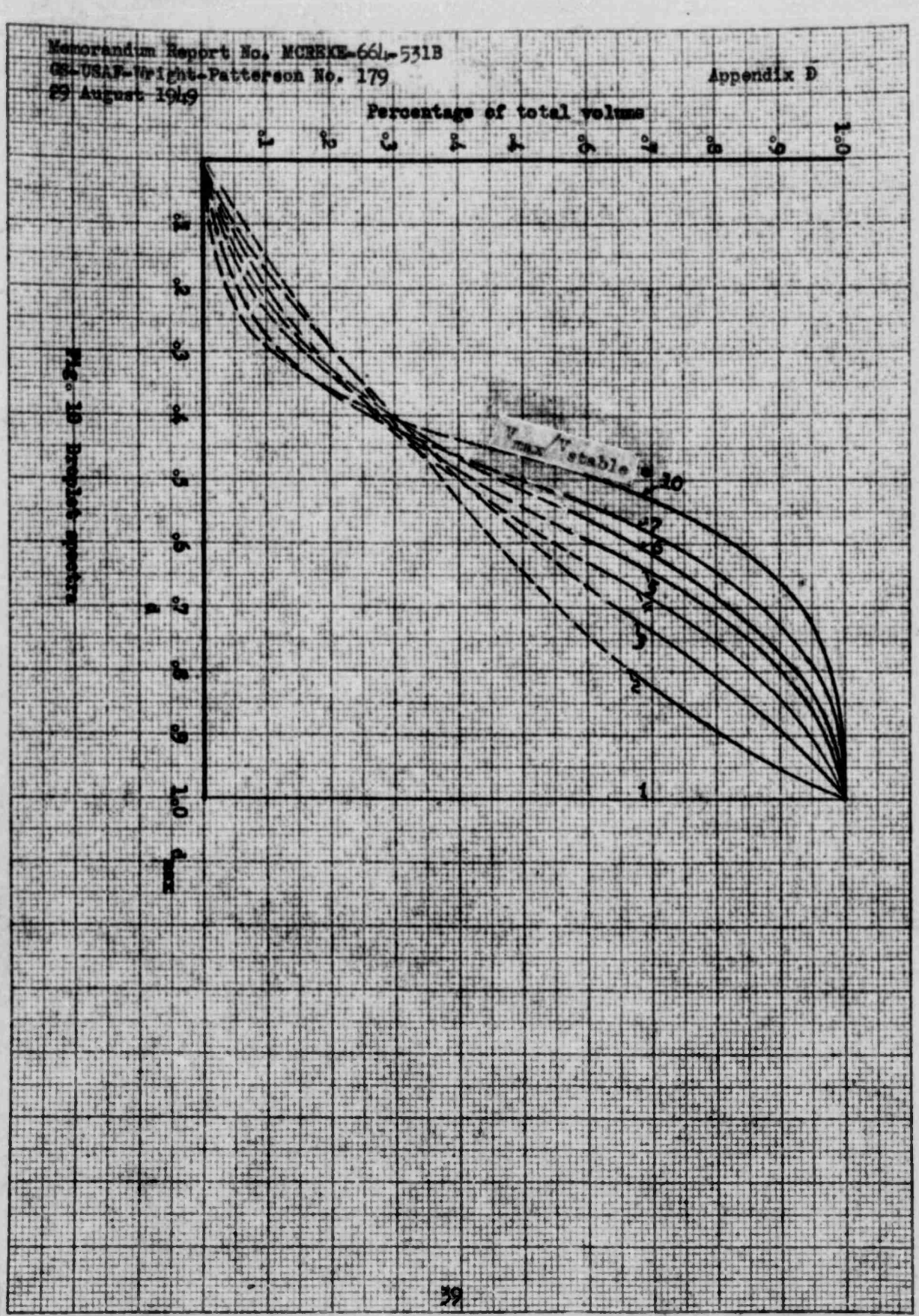

Appendix D

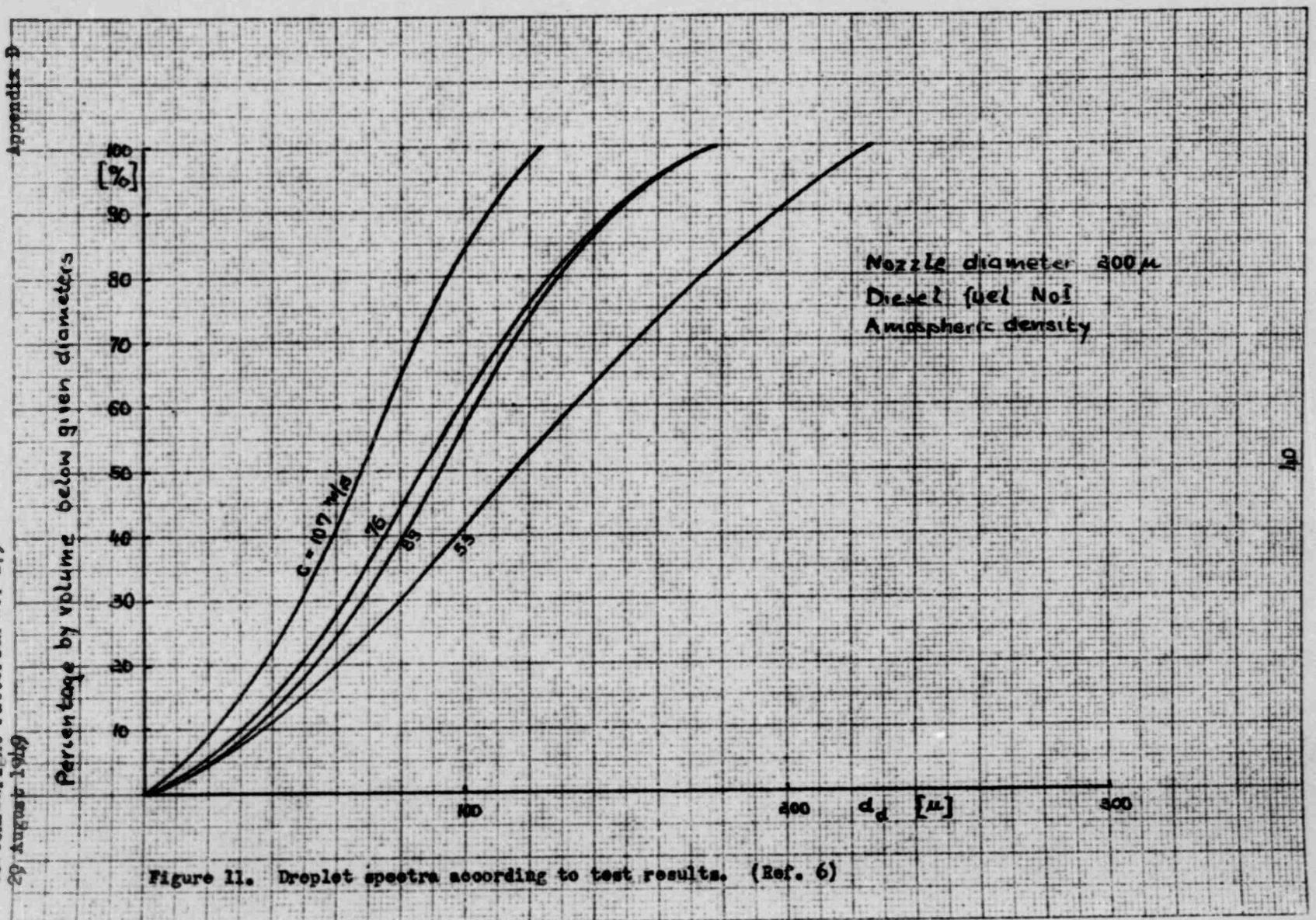

Figure 11. Droplet spectra according to test results. (Ref. 6)

Appendix D

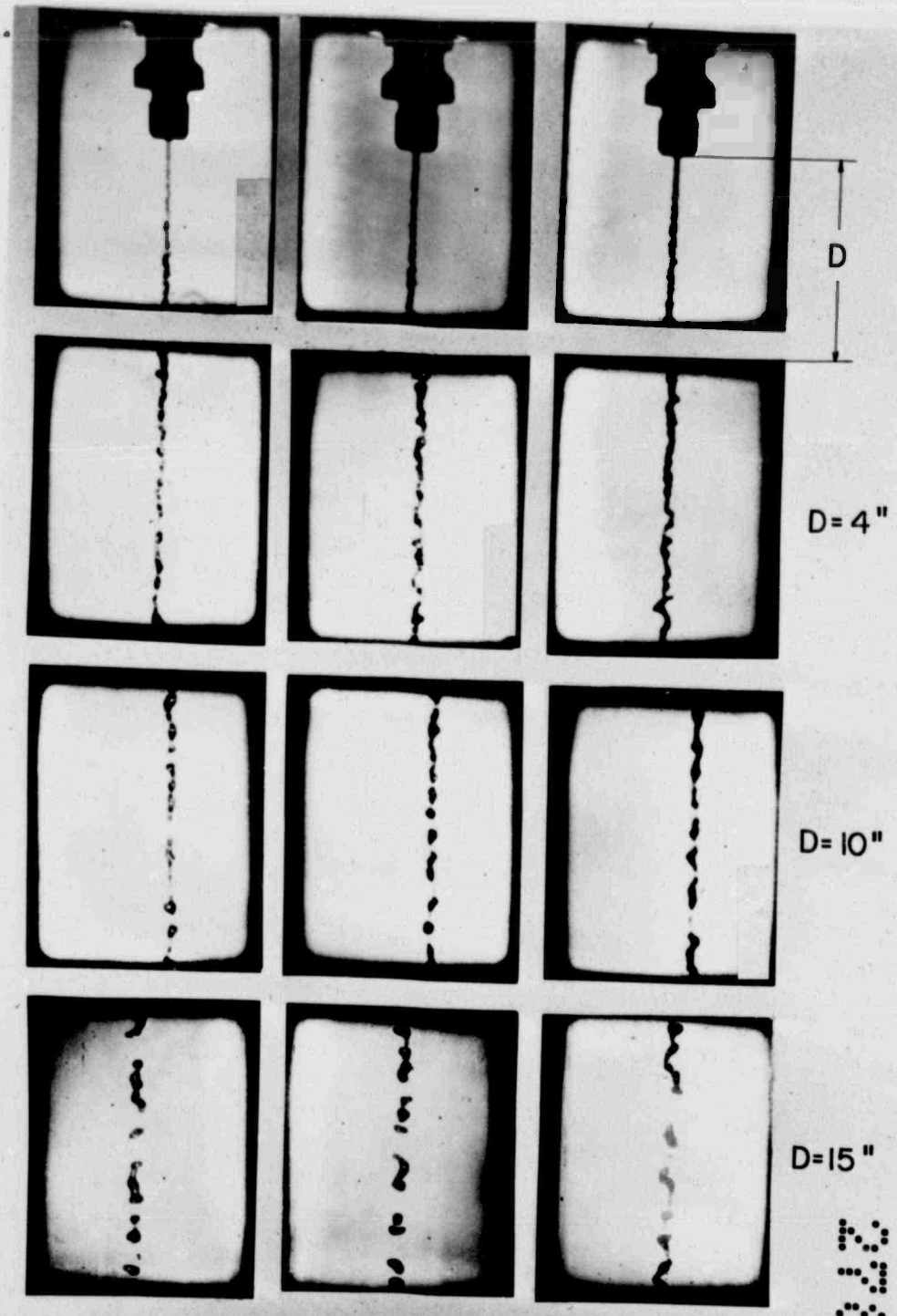

FIG.12A:DISINTEGRATING JET.

PICTURES BY COURTESY OF E.E.SOEHNGEN

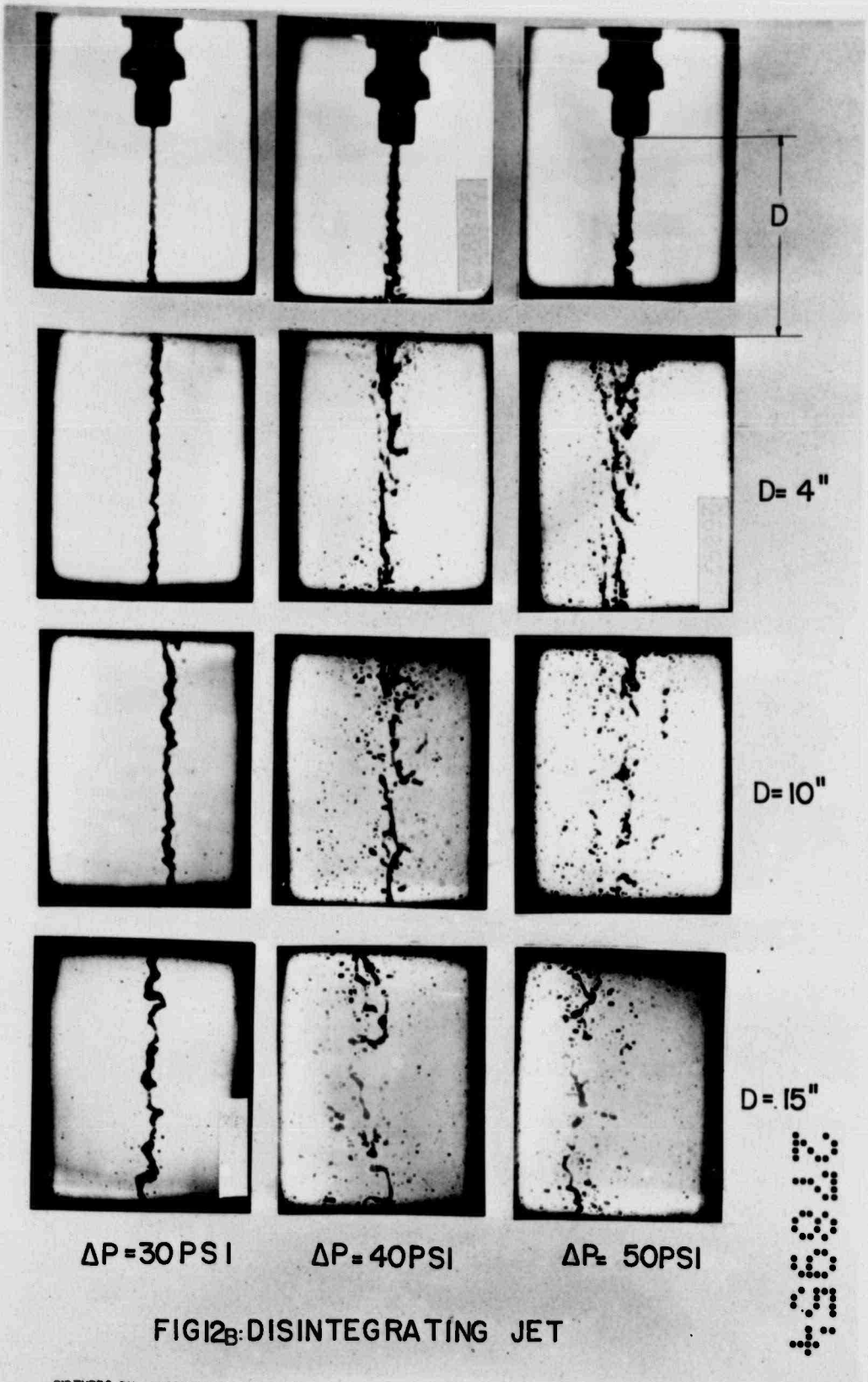

FIG12B: DISINTEGRATING JET

PICTURES BY COURTESY OF E.E.SOEHNGEN

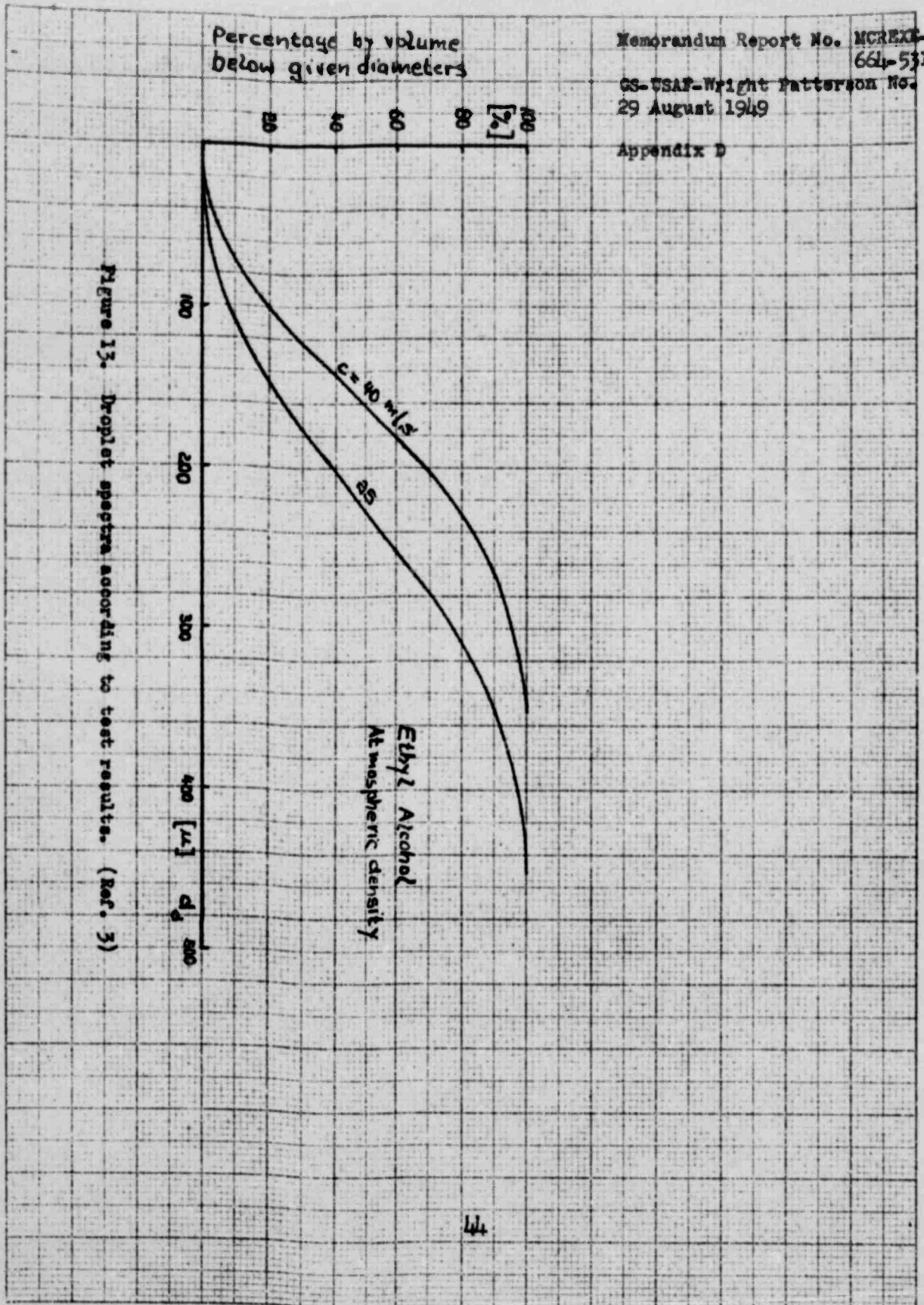

Figure 13. Droplet spectra according to test results. (Ref. 3)

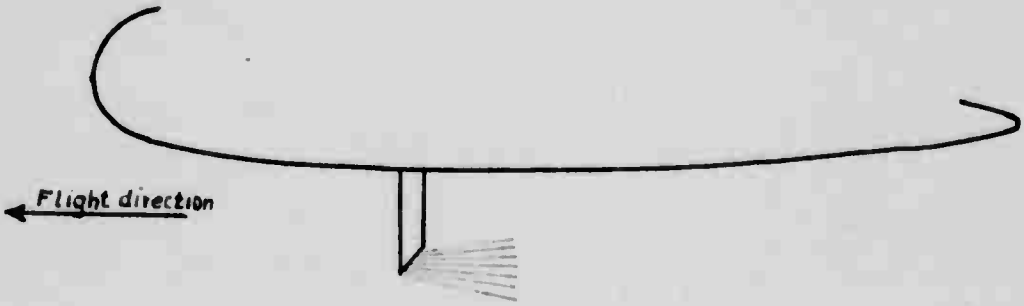

Fig. 14 Scetch of the straight discharge equipment

Memorandum Report No. MCREXE-664-531B
GE-USAF-Wright Patterson No. 179
29 August 1949

Appendix D

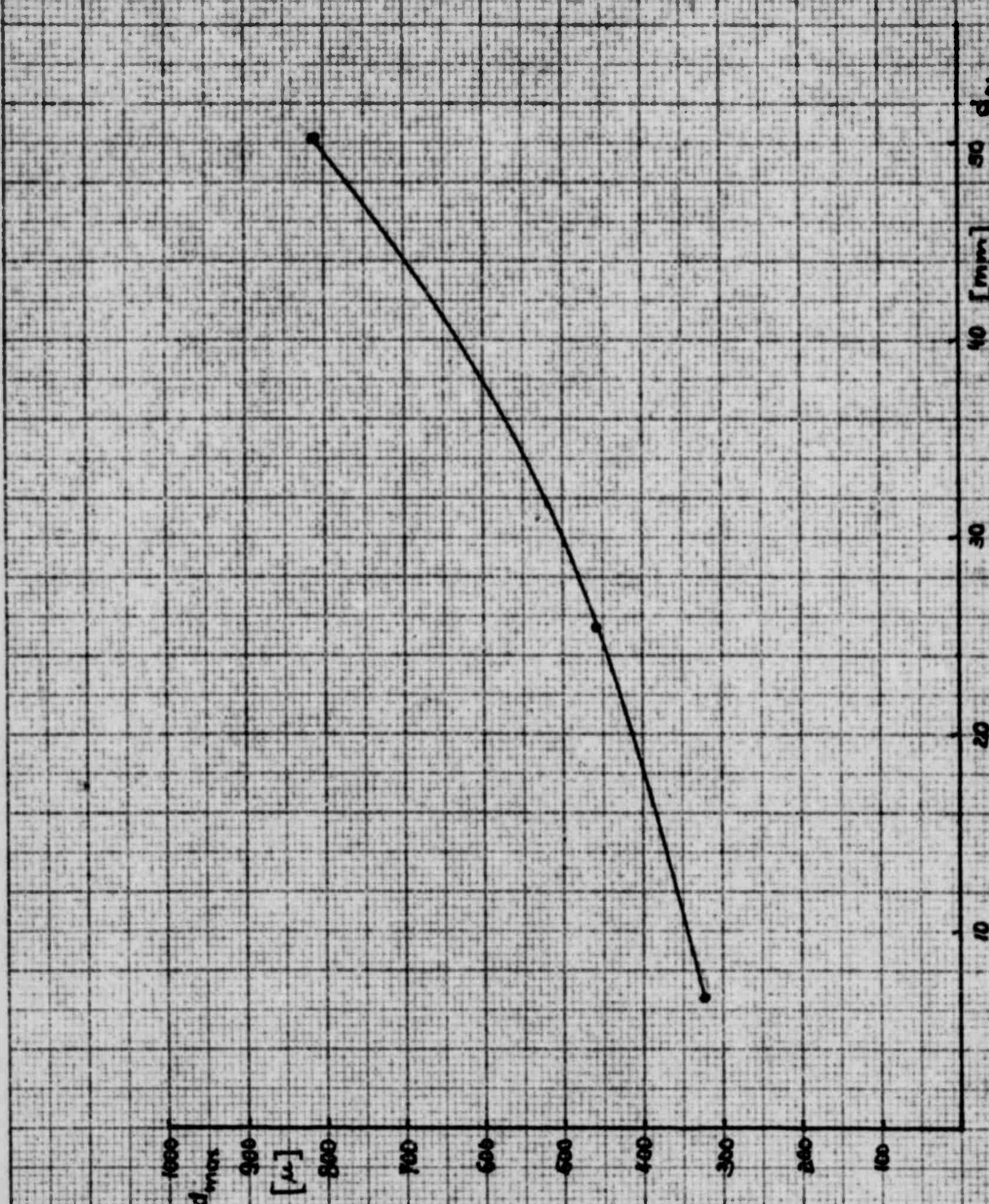

Figure 15. Test results obtained with straight discharge nozzle at flight velocity of 90 m/s.

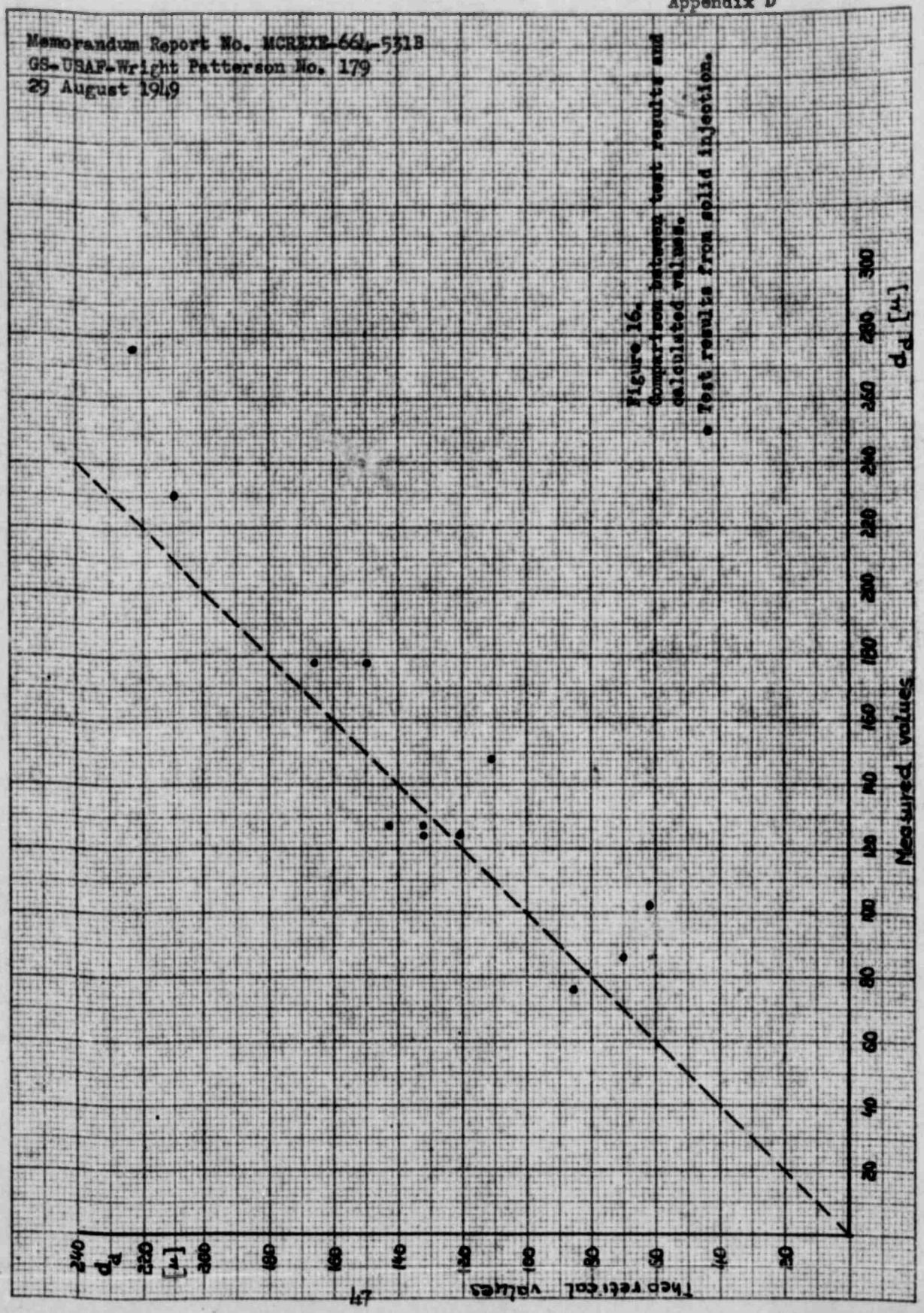

Figure 16.
Comparison between test results and calculated values.
• Test results from solid injection.

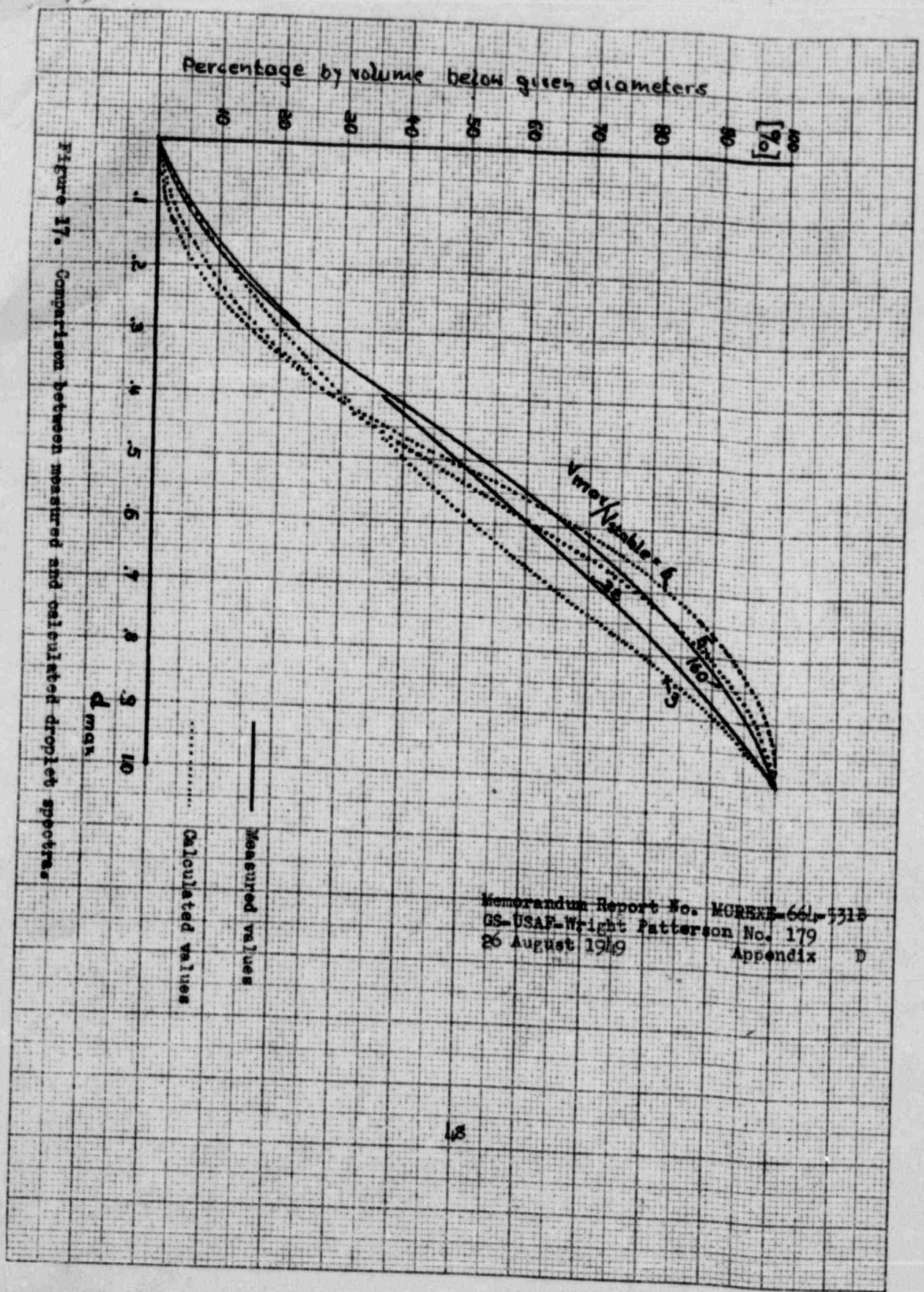

Figure 17. Comparison between measured and calculated droplet spectra.

TITLE: The Mechanism of Jet Disintegration - and Appendixes A-C

ATI- 64B10

REVISION (None)

AUTHOR(S) : Balje, O.E.; Larson, L.V.
ORIG. AGENCY : Engineering Division, Air Materiel Command
PUBLISHED BY : AMC, Wright-Patterson Air Force Base, Dayton, O.

ORIG. AGENCY NO. MCREXE 664-531B

PUBLISHING NO. (Same)

DATE	U.S. CLASS	COUNTRY	LANGUAGE	PAGES	ILLUSTRATIONS
Aug' 49	Unclass.	U.S.	English	48	photos, tables, graphs, drwgs

ABSTRACT:

An attempt was made to develop a theory about the mechanism of jet disintegration in order to derive mathematical relations for computing droplet sizes produced by insecticide spray equipment. The most important value for calculating the droplet sizes resulting from the disintergration of a liquid jet is the wave length originating in the liquid jet as a consequence of its instability.

DISTRIBUTION: ~~LIMITED, Route requests through AMC, Attn: MCREXE for approval.~~ ASTIA 1/14/58

DIVISION: Sciences, General (33)
SECTION: Physics (2)

SUBJECT HEADINGS: Drops, Liquid - Atomization
Jet stream - Flow measurement